

Lecture 2

Adiabatic potentials

The previous lecture was devoted to the basic ingredients of adiabatic potentials for rf-dressed atoms: spin transformations, spin interaction with static or rf fields, and the dressed state picture. We already discussed the effect of space dependence for a static magnetic field, which is used for magnetic trapping, and the finite lifetime due to non adiabatic transitions (Majorana losses). This lecture will introduce space dependence for the dressed atom in the presence of a rf field, which leads to an rf adiabatic potential. Only a few examples will be given, involving a limited number of experiments in a few groups.

1 Adiabatic potentials

In this lecture, the static magnetic field depends on position, like in a magnetic trap. It is easy to show from the Maxwell equations that if its amplitude depends on \mathbf{r} , its direction must also vary with position.¹ We have then $\mathbf{B}_0(\mathbf{r}) = B_0(\mathbf{r})\mathbf{u}(\mathbf{r})$. The local Larmor frequency is $\omega_0(\mathbf{r}) = |g_S|\mu_B B_0(\mathbf{r})/\hbar$.

1.1 Adiabatic energies

In addition to the static magnetic field, we introduce a rf field, oscillating at a frequency ω , chosen in the typical range of the Larmor frequency. At some particular positions, the Larmor frequency is exactly ω . The locus of the points such that $\omega_0(\mathbf{r}) = \omega$ is a surface in space, characterized by a given value of the magnetic field $B_0 = \hbar\omega/(|g_S|\mu_B)$, which we refer to as the *resonance surface*. This surface is determined by the choice of ω . It is often topologically equivalent to a sphere.

The system is described by the following hamiltonian:

$$\hat{H} = \frac{\hat{\mathbf{P}}^2}{2M} + \frac{g_s\mu_B}{\hbar} B_0(\hat{\mathbf{R}}) \hat{\mathbf{S}} \cdot \mathbf{u}(\mathbf{r}) + \left\{ \frac{g_s\mu_B}{\hbar} \frac{B_1(\hat{\mathbf{R}})}{2} e^{-i\varepsilon\omega t} \hat{\mathbf{S}} \cdot \boldsymbol{\epsilon}(\hat{\mathbf{R}}) + h.c. \right\}, \quad (1)$$

where we have taken a classical description for the field, with complex amplitude $B_1(\mathbf{r})$ and complex polarization $\boldsymbol{\epsilon}(\mathbf{r})$.

Assuming that the adiabatic approximation is valid, see Lecture 1, section 2, we will take a semi-classical approach to describe the atom and replace the positions and momentum operators by their average value \mathbf{r} and \mathbf{p} . At each fixed position \mathbf{r} , we can apply the procedure described in the last lecture to get the spin eigenstates and the eigenenergies:

¹Assume $\mathbf{B}_0(\mathbf{r}) = B_0(\mathbf{r})\mathbf{u}_z$. Then $\nabla \cdot \mathbf{B}_0 = 0 \Rightarrow \partial_z B_0 = 0$, while $\nabla \times \mathbf{B}_0 = 0 \Rightarrow \partial_x B_0 = 0$ and $\partial_y B_0 = 0$, which implies that B_0 is uniform.

apply a rotation of angle $\varepsilon\omega t$ around the axis $\mathbf{u}(\mathbf{r})$, apply the rotating wave approximation to remove counter-rotating terms, and diagonalize the effective, time-independent hamiltonian.

An important point is that the σ^ε polarization, which the only efficient component to couple spin state in the RWA, must be defined with respect to the local quantization axis $\mathbf{u}(\mathbf{r})$. Using the local spherical basis $(\mathbf{e}_+(\mathbf{r}), \mathbf{e}_-(\mathbf{r}), \mathbf{u}(\mathbf{r}))$, the relevant rf coupling is

$$\Omega_+(\mathbf{r}) = -\sqrt{2}\frac{g_s\mu_B}{\hbar}\frac{B_1(\mathbf{r})}{2}\mathbf{e}_+(\mathbf{r}) \cdot \boldsymbol{\epsilon}(\mathbf{r}). \quad (2)$$

It is clear from this expression that, even if the rf amplitude B_1 is homogeneous, the Rabi frequency is position dependent, because of the position dependent direction of the static magnetic field.

The eigenstates and their energies now depend on the local detuning $\delta(\mathbf{r}) = \omega - \omega_0(\mathbf{r})$ and on the local coupling $|\Omega_+(\mathbf{r})|$. The energy of the adiabatic state $|m\rangle_{\text{adia}}$ at a fixed point \mathbf{r} are

$$V_m(\mathbf{r}) = m\hbar\sqrt{\delta(\mathbf{r})^2 + |\Omega_+(\mathbf{r})|^2}. \quad (3)$$

They act as a potential for the atoms if the spin can follow the local eigenstate while the atom is moving.

In general, the maximally polarized state $|m = S\rangle_{\text{adia}}$ is used to trap atoms. For a spin 1 or 1/2, this is the only trappable state around the resonance point. For $S > 1$, this choice allows to suppress inelastic collisions: the spin of the atoms initially in a non fully polarized state can flip in a collision, and cause losses. The same is also true in a magnetic trap. One may wonder if this stays true for dressed spin, as the direction of the quantization field rotates at frequency ω . However, all the spins at the same location rotate in phase, and the collision is so quick that the quantization field can be considered fixed during the collision time. Polarizing the atoms in the extremal state $|m = S\rangle_{\text{adia}}$ is thus an efficient way to prevent inelastic collisions in an adiabatic potential [1].

In this adiabatic state $|m = S\rangle_{\text{adia}}$, the potential energy is always positive

$$V_S(\mathbf{r}) = S\hbar\sqrt{\delta(\mathbf{r})^2 + |\Omega_+(\mathbf{r})|^2}.$$

1.2 Bubble traps

To understand better the shape of the adiabatic potential, let us first assume that the rf effective coupling $|\Omega_+(\mathbf{r})|$ is homogeneous and equal to Ω . This is relevant if the direction of the static field varies only slightly close to the potential minimum of the adiabatic potential. It is then clear that, in the absence of gravity, the potential is minimum where $\delta(\mathbf{r}) = 0$, that is on the isomagnetic resonant surface defined by $\omega_0(\mathbf{r}) = \omega$. This provides us with very anisotropic traps, where one direction transverse to the isomagnetic surface is confined, and may be strongly confined, by the avoided crossing of the adiabatic potential, while the directions parallel to the surface are free to move.

How much are the atoms indeed confined to an isomagnetic surface $\delta(\mathbf{r}) = 0$? Let us evaluate the strength of this. By definition, the direction normal to the surface is given by the gradient of the Larmor frequency $\nabla\omega_0$. Along this direction, locally, the variations of ω_0 are linear, and so are the variations of δ : $\delta(\mathbf{r} + \Delta\mathbf{r}) \simeq \Delta\mathbf{r} \cdot \nabla\omega_0$. We can expand

V_S around \mathbf{r} to determine the oscillation frequency in the harmonic approximation in the direction $\nabla\omega_0$ normal to the surface. We find:

$$\omega_{\text{transverse}} = \alpha \sqrt{\frac{S\hbar}{M\Omega}}, \quad (4)$$

where $\alpha = |\nabla\omega_0|$ is the local magnetic gradient in units of frequency. This formula is analogous than the one giving the largest of the two frequencies of a cigar-shape Ioffe-Pritchard trap. However, here the Larmor frequency appearing in the denominator, and typically of order 1 MHz, is replaced by the Rabi frequency, typically between 20 and 200 kHz. For a similar magnetic gradient, the confinement to the isomagnetic surface in an adiabatic potential is thus significantly larger than what is obtained in a IP trap. The transverse confinement frequency is typically in the range of a few kHz. We can thus have a good idea of the trap geometry by assuming that the atoms will be confined to the isomagnetic surface. The effect of the position dependence of $|\Omega_+(\mathbf{r})|$ or of gravity is essentially to shape a refined landscape inside this surface.

If the static magnetic field $B(\mathbf{r})$ has a local minimum B_{min} , as it is the case in a magnetic trap, the isomagnetic surfaces close to this minimum are typically ellipsoids (a trap is generally harmonic close to its minimum). This is the basic idea for a bubble trap, as proposed by Zobay and Garraway [2, 3] and first realized by Colombe et al. [4], see Fig. 1.

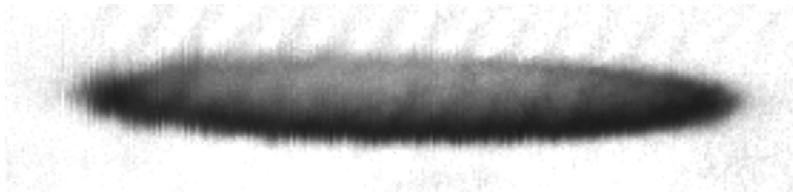


Figure 1: Cold rf-dressed atoms confined in an adiabatic potential. The static magnetic field comes from a cigar shape Ioffe-Pritchard trap. Atoms are spread around an ellipsoid, isomagnetic surface of the magnetic static field. The atomic density is higher at the bottom of the ellipsoid, where gravity pulls the atoms. Figure from O. Morizot's thesis [5].

When gravity is included, the isomagnetic surface is no longer an isopotential of the total potential $V_{\text{tot}}(\mathbf{r}) = S\hbar\sqrt{\delta(\mathbf{r})^2 + |\Omega_+|^2} + Mgz$. There is a single minimum, at the bottom of the ellipsoid. Depending on the energy of the cloud, which for thermal atoms is their temperature, the atoms will fill the bubble up to a certain height given by the barometric energy: $h_{\text{max}} \sim k_B T / (Mg)$. For a Bose-Einstein condensate, the relevant energy scale is the chemical potential and $h_{\text{max}} \sim \mu / (Mg)$.

The radii of the resonant ellipsoid can be adjusted with the choice of the rf frequency ω . Increasing ω from the minimum Larmor frequency in the trap center $\omega_{0,\text{min}}$ makes the bubble inflate, so that the z radius becomes larger than h_{max} at some point. Above this frequency, the atoms are confined to a curved plane. The pictures of Fig. 2 show ultra cold atoms confined in such an anisotropic trap, for various values of the dressing frequency ω .

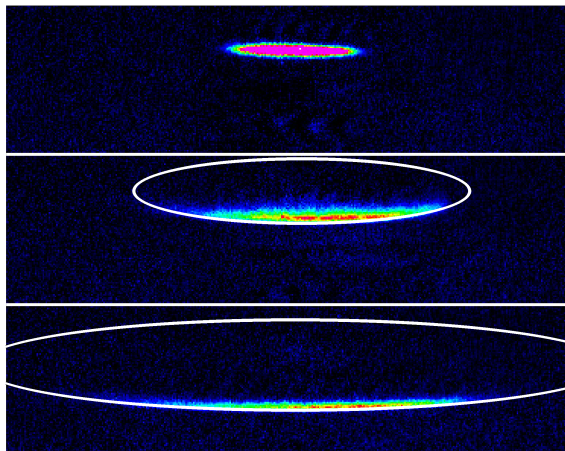


Figure 2: Cold rf-dressed atoms confined in an adiabatic potential, for different values of the dressing frequency [4]. Top: no rf dressing, atoms are trapped in a Ioffe-Pritchard trap with a cigar shape. The Larmor frequency at the trap bottom is 1.3 MHz. Middle: rf dressing field at 3 MHz. The atoms occupy the lower part of a bubble. The field of view is 4.5 mm (horizontally) \times 1.2 mm (vertically). The center of mass is shifted vertically by 130 μm . Lower picture: dressing frequency 8 MHz. The isomagnetic bubble is larger, the atoms are more shifted (by 450 μm) and the cloud is even more anisotropic. The resonant isomagnetic surfaces are marked with a white line. Figure from O. Morizot's thesis [5].

1.3 Loading from a magnetic trap

Adiabatic potentials could in principle be loaded from a MOT, like magnetic traps. However, their trapping volume is in general much smaller, as the interesting feature of the large anisotropy also comes with a small volume. Moreover, spin flips can occur at high temperature (a few tens of μK) because the relevant effective splitting frequency is Ω , of order 100 kHz, in general smaller than the minimum Larmor frequency $\omega_{0,\text{min}}$ in a magnetic trap, of order 1 MHz. Adiabatic potentials are very well adapted to trap ultra cold atoms or condensates, pre-cooled by evaporative cooling in a magnetic trap.

The loading procedure from a magnetic trap presenting a non zero Larmor frequency $\omega_{0,\text{min}}$ at its bottom is straightforward, and is sketched on Fig. 3. The idea is to operate a frequency sweep from an initial frequency below $\omega_{0,\text{min}}$, up to the desired final value above $\omega_{0,\text{min}}$, in the spirit of the frequency sweep described in section 3.2 of Lecture 1. The rf field is switched on at a fixed negative detuning $\delta = \omega - \omega_{0,\text{min}}$, in a time sufficiently long to ensure the adiabatic condition $\dot{\Omega} \ll \delta^2$. The initial, trapped, upper magnetic state $|\varepsilon S\rangle_z$ is connected to the upper dressed state $|S\rangle_{\mathbf{u}}$. When the rf frequency is subsequently increased, the atoms stay in this upper adiabatic state if the ramp is slow, so that $\dot{\delta} \ll \Omega^2$. Once ω reaches $\omega_{0,\text{min}}$, the atoms have reached the resonant surface, and they remain at this surface, which is now a potential minimum, as the rf frequency is further increased.

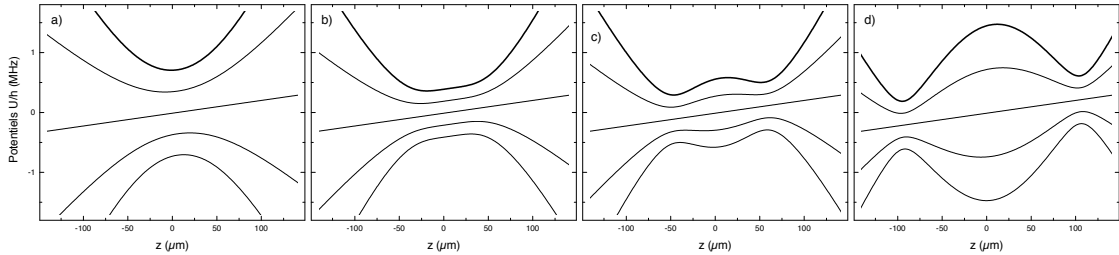


Figure 3: Loading procedure from a magnetic trap with non zero minimum. The adiabatic potentials are represented for the five states of a $S = 2$ spin, along the vertical axis. Gravity is included. From left to right, the rf frequency is ramped from below resonance to the final value. The atoms start in the upper potential, which is the same as the magnetic trapping potential for the leftmost picture. The second picture corresponds to the resonance at the bottom of the trap, $\omega = \omega_{0,\min}$. Above $\omega_{0,\min}$, there is a single trap minimum at the bottom of the ellipsoid, due to gravity, which position z changes with the dressing frequency. Figure from Y. Colombe’s thesis [6].

1.4 Phase jumps, frequency jumps

Phase or frequency jumps during the loading ramp leads to trap losses. The phase should be continuous, and DDS² devices are preferred to generate the rf source. The ramp is done by a number of small frequency steps. Each step should be kept very small to prevent losses by spin projection onto the new, different axis. See details in Ref. [7], where you will also find an analysis on the possible sources of heating.

2 Effect of the rf polarization: from tube to double well

2.1 Isomagnetic surfaces

The simplified view of a uniform $|\Omega_+(\mathbf{r})|$ is often not sufficient to describe correctly the adiabatic potential. In some cases, the trap geometry is strongly modified by an inhomogeneous effective coupling due to the inhomogeneity of the magnetic field orientation. If $|\Omega_+|$ varies faster than δ with position, the position of the trap minimum can be governed by the position of the coupling minimum. Most of the time, however, the variation in δ is faster, so that the atoms stay within the resonant surface. The shape of the trap is nevertheless strongly affected by either gravity or a variation of $|\Omega_+(\mathbf{r})|$ within the resonant surface. In this section, we describe an atom chip experiment which took advantage of this effect to realize a double well potential.

The static magnetic field we start from is again a Ioffe-Pritchard magnetic trap. Let us write explicitly the magnetic field in this trap:

$$\mathbf{B}_0(\mathbf{r}) = (B_{\min} + \frac{b''}{2}z^2) \mathbf{e}_z + b'(x \mathbf{e}_x - y \mathbf{e}_y) = B_z(z) \mathbf{e}_z + b'(x \mathbf{e}_x - y \mathbf{e}_y).$$

²Direct Digital Synthesis

Its modulus is

$$B_0(\mathbf{r}) = B_{\min} \left[1 + \frac{b''}{2B_{\min}} z^2 + \frac{b'^2}{2B_{\min}^2} (x^2 + y^2) \right] = B_0(\rho, z)$$

up to second order in x, y, z , giving rise to a cylindrically symmetric cigar-shape harmonic trapping near the center, with frequencies $\omega_x = \omega_y \gg \omega_z$. Away from the z axis, where $\rho = \sqrt{x^2 + y^2} \ll B_{\min}/b'$, the trap is closer to a linear potential, with $B_0(\mathbf{r}) \simeq b'\rho$.

Frequency units are sometimes more convenient. The Larmor frequency is denoted $\omega_0(\rho, z)$, with a minimum value ω_{\min} at the centre, and the gradient in frequency units is $\alpha = |g_S|\mu_B b'/\hbar$. We also define $\eta = |g_S|\mu_B b''/\hbar$, the curvature in units of frequency. We can then also write

$$\omega_0(\rho, z) = \omega_0(0, z) + \frac{\alpha^2}{2\omega_{\min}} \rho^2, \quad \text{with} \quad \omega_0(0, z) = \omega_{\min} + \frac{1}{2}\eta z^2.$$

The resonant surface is defined by $\omega_0(\rho_{\text{res}}(z), z) = \omega$. At each longitudinal position z , the resonant radius ρ_{res} is given by

$$\rho_{\text{res}}(z) = \frac{1}{\alpha} \sqrt{\omega^2 - \left(\omega_{\min} + \frac{\eta z^2}{2} \right)^2}. \quad (5)$$

It depends only slowly on z . For $\omega \sim \omega_{\min}$, the maximum radius $\rho_0 = \rho_{\text{res}}(0)$ scales like $\sqrt{\omega - \omega_{\min}}$. For rf frequencies much larger than ω_{\min} , the dependence becomes linear:

$$\rho_0 \simeq \frac{\omega}{\alpha} \quad \text{for} \quad \omega \gg \omega_{\min}.$$

Tuning the frequency is thus a natural and efficient way to increase the radius of the isomagnetic surface.

2.2 Local circular polarization

Near the magnetic trap bottom, the axis of the magnetic field is close to \mathbf{e}_z . It is then natural to chose for the rf field a polarization which is either σ^+ or σ with respect to this axis. We assume that the rf field is homogeneous, in amplitude and polarization. The rf magnetic field reads

$$\mathbf{B}_1 = \frac{B_1}{2} \boldsymbol{\epsilon} e^{-i\omega t} + c.c.$$

where $\boldsymbol{\epsilon}$ is a complex polarization. We must find the projection of this field onto the local σ^+ polarization, the quantization axis being

$$\mathbf{u} = \frac{B_z(\mathbf{r})}{B_0(\mathbf{r})} \mathbf{e}_z + \frac{b'x}{B_0(\mathbf{r})} \mathbf{e}_x - \frac{b'y}{B_0(\mathbf{r})} \mathbf{e}_y.$$

It is convenient to introduce a new basis, adapted to this problem. Let \mathbf{v} and \mathbf{w} be defined as

$$\mathbf{v} = \frac{x}{\rho} \mathbf{e}_x - \frac{y}{\rho} \mathbf{e}_y \quad \mathbf{w} = \frac{y}{\rho} \mathbf{e}_x + \frac{x}{\rho} \mathbf{e}_y.$$

$(\mathbf{v}, \mathbf{w}, \mathbf{e}_z)$ is an orthonormal basis. In this basis, \mathbf{u} writes

$$\mathbf{u} = \frac{B_z(\mathbf{r})}{B_0(\mathbf{r})} \mathbf{e}_z + \frac{b'\rho}{B_0(\mathbf{r})} \mathbf{v}.$$

It is the transformed of \mathbf{e}_z by a certain rotation around \mathbf{w} . The same rotation doesn't affect \mathbf{w} , and transforms \mathbf{v} into

$$\mathbf{v}' = -\frac{b'\rho}{B_0(\mathbf{r})} \mathbf{e}_z + \frac{B_z(\mathbf{r})}{B_0(\mathbf{r})} \mathbf{v}.$$

With respect to the local direction of the magnetic field \mathbf{u} , the σ^+ polarization is thus defined, apart from a global phase factor, as

$$\mathbf{e}_{+, \mathbf{u}} = -\frac{1}{\sqrt{2}} (\mathbf{v}' + i\mathbf{w}).$$

The effective Rabi frequency is then deduced from the scalar product $\mathbf{e}_{+, \mathbf{u}}^* \cdot \boldsymbol{\epsilon}$.

2.3 Circular polarization

For a circular rf polarization along z , $\boldsymbol{\epsilon} = -\frac{1}{\sqrt{2}} (\mathbf{e}_x + i\mathbf{e}_y)$ and we find

$$B_+^{\sigma^+} = \frac{B_1}{4} \left[\frac{B_z}{B_0} \frac{x}{\rho} + \frac{x}{\rho} + i \left(-\frac{B_z}{B_0} \frac{y}{\rho} - \frac{y}{\rho} \right) \right] = \frac{B_1}{4} \left(1 + \frac{B_z}{B_0} \right) \frac{x - iy}{\rho}.$$

$$|B_+| = \frac{B_1}{4} \left(1 + \frac{B_z(z)}{B_0(z, \rho)} \right).$$

Defining Ω as the maximum coupling, corresponding to $\hbar\Omega = |g_S| \mu_B B_1 / 2$, we have

$$|\Omega_+(\mathbf{r})| = |\Omega_+(\rho, z)| = \frac{\Omega}{2} \left[1 + \frac{\omega_0(0, z)}{\omega_0(\rho, z)} \right].$$

The rf coupling reaches its maximum Ω on the z axis, and is reduced as ρ increases. The coupling does not depend on the polar angle θ , and the rotational invariance of the IP potential is preserved. On the resonance surface $\omega_0 = \omega$, the rf coupling is

$$|\Omega_+(\rho, z)| = \frac{\Omega}{2} \left[1 + \frac{\omega_0(0, z)}{\omega} \right].$$

The bubble geometry described at section 1.2 is not much changed, see Fig. 4, left. Because of the reduction of the coupling with increasing ρ , the potential minimum is simply shifted very slightly to a larger radius with respect to the resonant radius $\rho_{\text{res}}(z)$. Along z , on the resonance surface, the minimum coupling is obtained for $z = 0$. If one can manage to compensate for gravity, the total potential is ring shaped, or more precisely tubular, because it is very elongated along z [8].

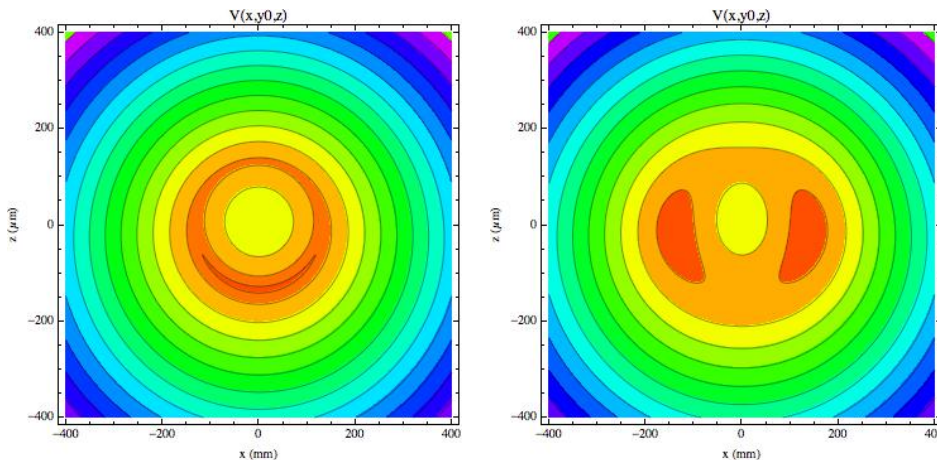


Figure 4: Isopotential lines in the ring trap (left) and the double well trap (right), seen in the xy plane. Gravity is along y and is taken into account.

2.4 Linear polarization

The situation is quite different for a linear (σ) polarization. If gravity is along the y axis, let us consider a rf field polarized along x : $\epsilon = \mathbf{e}_x$. The effective rf amplitude is

$$B_+^\sigma = \frac{B_1}{2\sqrt{2}} \left[-\frac{B_z}{B_0} \frac{x}{\rho} + i \frac{y}{\rho} \right]$$

$$|B_+^\sigma| = \frac{B_1}{2\sqrt{2}} \left[\frac{B_z^2}{B_0^2} \frac{x^2}{\rho^2} + \frac{y^2}{\rho^2} \right] = \frac{B_1}{2\sqrt{2}} \left[1 - \frac{b^2 x^2}{B_0^2} \right].$$

The coupling is lower on the x axis than on the y axis, by a factor B_z^2/B_0^2 . On the resonant surface $\rho = \rho_{\text{res}}(z)$, the effective Rabi coupling is thus

$$|\Omega_+| = \Omega \left[1 - \frac{\alpha^2 x^2}{\omega^2} \right], \quad |x| \leq \rho_{\text{res}}(z)$$

where Ω is the maximum coupling, reached in the $x = 0$ plane. $|\Omega_+|$ is minimum for $y = 0$ and $x = \rho_{\text{res}}(z)$, for which $|\Omega_+| = \Omega [\omega_0(0, z)/\omega]^2$. The absolute coupling minimum is thus $|\Omega_+| = \Omega [\omega_{\text{min}}/\omega]^2$, obtained at the two equatorial positions $(\pm\rho_0, 0, 0)$.

Let us look for the potential minimum inside the resonant surface. Because of the reduced coupling at these points, in the absence of gravity, the potential has two minima, located at $x = \pm\rho_0, y = 0, z = 0$, see Fig. 4, right. The energy at these points is $S\hbar\Omega [1 - (\alpha\rho_0/\omega)^2]$, to be compared to the highest energy points at $x = 0, y = \pm\rho_{\text{res}}(z)$ where the energy is $S\hbar\Omega$. The energy difference due to the inhomogeneity in the rf coupling is equal to $S\hbar\Omega (\alpha\rho_0/\omega)^2$.

As discussed in section 2.1, the resonant radius ρ_0 is tuned by changing the rf frequency. For $\omega \sim \omega_{\text{min}}$, the maximum radius ρ_0 scales like $\sqrt{\omega - \omega_{\text{min}}}$. For rf frequencies much larger than ω_{min} , $\rho_0 \simeq \omega/\alpha$. It is then straightforward to adjust at will the distance $2\rho_0$ between the two wells by tuning the rf frequency, which has been done to perform atom interferometry on a chip [9], see Fig. 5.

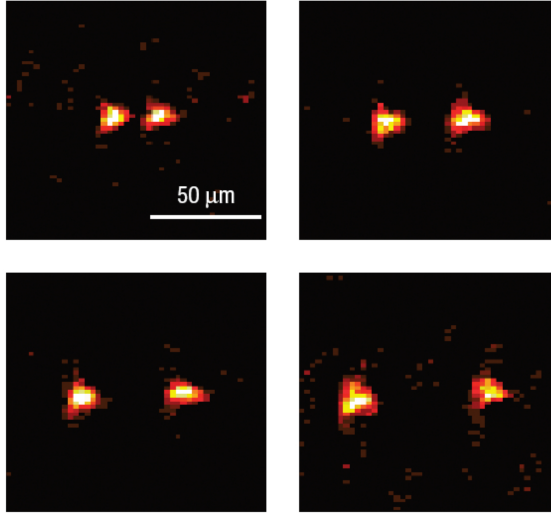


Figure 5: First experimental realization of the rf double well trap [9]. The distance between two Bose-Einstein condensates in elongated traps is adjusted with the rf frequency.

We must now discuss the effect of gravity, which in the case of the tubular potential would significantly change the shape of the minimum if it is not compensated. Here, gravity won't affect qualitatively the double well trap if the energy difference is produced between the equator and the bottom of the resonant surface is less pronounced than the rf coupling difference, that is if

$$Mg\rho_{\text{res}} < S\hbar\Omega\frac{\alpha^2\rho_{\text{res}}^2}{\omega^2}. \quad (6)$$

To discuss if this relation is fulfilled, we introduce the parameter $\beta = S\frac{\hbar\alpha}{Mg}$, which is the ratio between the magnetic force and the gravity force. It has to be larger than one, for the IP trap to confine atoms against gravity. The condition (6) can be written using β as:

$$1 < \beta\frac{\alpha\rho_{\text{res}}}{\omega}\frac{\Omega}{\omega}.$$

The ratio $\alpha\rho_{\text{res}}/\omega$ is always less than one, see Eq.(5), and reaches one in the limit where $\omega \gg \omega_{\text{min}}$. The condition (6) is then fulfilled for all double well distances if

$$1 < \beta\frac{\Omega}{\omega}, \quad \text{or} \quad \omega < \beta\Omega. \quad (7)$$

If we want to stay in the RWA where $\Omega \ll \omega$, the magnetic gradient must be much stronger than gravity, $\beta \gg 1$. This explains why atom chips are ideal devices for these double well trap, as they provide us with large magnetic gradients.

3 The dressed quadrupole trap

Another interesting case, which allows to obtain very flat traps for 2D quantum gases, is the adiabatic potential obtained from dressing atoms in a quadrupole field [10, 11]. We

will discuss this trap here.

3.1 Magnetic field geometry

The magnetic field is linear in the position, for example:

$$\mathbf{B}_0(\mathbf{r}) = b'(x \mathbf{e}_x + y \mathbf{e}_y - 2z \mathbf{e}_z). \quad (8)$$

The factor 2 in the z gradient ensure a vanishing divergence of the magnetic field. The corresponding Larmor frequency is

$$\omega_0(\mathbf{r}) = \alpha \sqrt{x^2 + y^2 + 4z^2}, \quad (9)$$

where $\alpha = |g_S| \mu_B b' / \hbar$.

The isomagnetic surfaces in this case are ellipsoids, with a radius smaller in the vertical direction by a factor of two. For a given rf frequency ω , the equation of the resonant ellipsoid is

$$x^2 + y^2 + 4z^2 = r_0^2,$$

where the ellipsoid horizontal radius is related to the frequency through

$$r_0 = \frac{\omega}{\alpha}. \quad (10)$$

The naive potential, forgetting polarization issues, is thus a bubble, the atoms being attracted to its bottom by gravity. This explains why this configuration is well adapted to the trapping of two-dimensional gases.

3.2 Local basis

Again, in order to determine the adiabatic potential, we need to know the local \mathbf{e}_+ vector. The direction of the magnetic field is given by

$$\mathbf{u} = \frac{\rho \mathbf{e}_\rho - 2z \mathbf{e}_z}{\sqrt{\rho^2 + 4z^2}}. \quad (11)$$

ρ is the polar coordinate in the xy plane, $\rho \mathbf{e}_\rho = x \mathbf{e}_x + y \mathbf{e}_y$. In the following, we will use the generalized distance to the center of the quadrupole,

$$\ell(\rho, z) = \sqrt{\rho^2 + 4z^2}. \quad (12)$$

In order to write the local circular polarization, we will use the orthogonal basis $(\mathbf{u}, \mathbf{u}_\theta, \mathbf{u}_\phi)$ defined by

$$\mathbf{u} = \frac{\rho \mathbf{e}_\rho - 2z \mathbf{e}_z}{\ell}, \quad (13)$$

$$\mathbf{u}_\theta = -\frac{2z \mathbf{e}_\rho + \rho \mathbf{e}_z}{\ell}, \quad (14)$$

$$\mathbf{u}_\phi = \frac{-y \mathbf{e}_x + x \mathbf{e}_y}{\rho}. \quad (15)$$

The unitary vector for the relevant circular polarization is thus

$$\begin{aligned}\mathbf{e}_+ &= -\frac{1}{\sqrt{2}}(\mathbf{u}_\theta + i\mathbf{u}_\phi) = \frac{1}{\sqrt{2\rho\ell}}(\rho^2\mathbf{e}_z + 2z\rho\mathbf{e}_\rho + i\ell y\mathbf{e}_x - i\ell x\mathbf{e}_y). \\ \mathbf{e}_+ &= \frac{1}{\sqrt{2\rho\ell}}[\rho^2\mathbf{e}_z + (2zx + i\ell y)\mathbf{e}_x + (2zy - i\ell x)\mathbf{e}_y].\end{aligned}\quad (16)$$

3.3 Circular polarization

The magnetic field at the bottom of the ellipsoid $(0, 0, -r_0/2)$ is aligned along the $+z$ axis. It is then natural to consider first a circularly polarized field. We will assume, to avoid heavy notation, that g_S is positive. To maximize the coupling at the bottom, we will hence chose a positive circular polarization aligned with z :

$$\boldsymbol{\epsilon} = -\frac{1}{\sqrt{2}}(\mathbf{e}_x + i\mathbf{e}_y).$$

The efficient Rabi component is then

$$\begin{aligned}\Omega_+ &= \Omega\mathbf{e}_+^* \cdot \boldsymbol{\epsilon} = -\frac{\Omega}{2\rho\ell}(2zx - i\ell y + 2izy - \ell x) = \frac{\Omega}{2\rho\ell}(x + iy)(\ell - 2z). \\ |\Omega_+| &= \frac{\Omega}{2}\left(1 - \frac{2z}{\ell}\right).\end{aligned}\quad (17)$$

Ω is the maximum Rabi frequency, obtained as expected on the negative side of the z axis, where $\ell = -2z$. On the other hand, the effective coupling vanishes on the positive side of the z axis, where $\ell = 2z$. The polarization here is σ^- with respect to the orientation of the magnetic field, which points downwards. This results on a half axis of zero coupling. The trap minimum must lie away from this $+z$ axis, in order to prevent spin flips.

The total potential, including gravity, in the extremal state $m = S$ is

$$V(\mathbf{r}) = S\hbar\sqrt{[\alpha\ell(\rho, z) - \omega]^2 + \frac{\Omega^2}{4}\left[1 - \frac{2z}{\ell(\rho, z)}\right]^2} + Mgz. \quad (18)$$

We can immediately notice that the potential is rotationally invariant around z , and depends only on ρ and z . The first term will be minimum when both the square detuning and the square coupling vanish, at the point $(0, 0, r_0/2)$. However, this is the point of the resonant surface where gravity is maximum, and it will help bringing the atoms to the bottom of the ellipsoid, away from the region of vanishing Rabi frequency.

Again, it is reasonable to assume that the minimum will lie on the resonance surface, which allows to set δ to zero. Let us write the value of the potential for atoms living on the two-dimensional resonance surface $\ell(\rho, z) = r_0$. It depends only on z now, as ρ is given by z and r_0 :

$$V_{\text{surf}}(z) = S\hbar\frac{\Omega}{2}\left(1 - \frac{2z}{r_0}\right) + Mgz, \quad |z| < \frac{r_0}{2}.$$

The potential on the surface is linear in z .

From this expression, it is clear that there will be a competition between the gradient of rf coupling and gravity. Let us use the same parameter $\beta = S\frac{\hbar\alpha}{Mg}$ as in section 2.4. It

has to be larger than one if the quadrupole field itself is supposed to confine atoms against gravity. If $Mgr_0 > S\hbar\Omega$, that is for $\omega > \beta\Omega$, gravity is dominant and the minimum is at $z = -r_0/2$, at the bottom of the ellipsoid where the coupling is maximum. On the other hand, if $\omega < \beta\Omega$, the atoms are pushed upwards to the point of the ellipsoid where the coupling vanishes, and the trap is unstable with respect to Landau-Zener losses. For a given coupling, this sets a minimum frequency which should be used:

$$\omega > \beta\Omega. \quad (19)$$

In contrast to the requirement for a double well, this is now easily compatible with RWA, which requires $\omega \gg \Omega$. The trap is thus normally at the bottom of the ellipsoid, even for moderate gradients.

3.4 Isotropic trap for a 2D gas

Let us assume that we have indeed $\omega > \beta\Omega$. In the vicinity of the bottom of the resonant surface, we can develop the full potential to find the oscillation frequencies. In the vertical direction, the trap is similar to the radial direction of a Ioffe Pritchard magnetic trap:

$$V(0, 0, z) = S\hbar\sqrt{\alpha^2 \left(z + \frac{r_0}{2}\right)^2 + \Omega^2} + Mgz \simeq S\hbar\Omega + Mgz + S\hbar\frac{\alpha^2}{2\Omega} \left(z + \frac{r_0}{2}\right)^2.$$

The vertical oscillation frequency is thus

$$\omega_z \simeq \alpha\sqrt{\frac{S\hbar}{M\Omega}}. \quad (20)$$

A corrections to this expression arises because the minimum does not strictly belongs to the resonant surface, due of gravity [11]. The analogy with the Ioffe Pritchard trap is immediate: the Larmor frequency is just replaced by the Rabi frequency. By analogy with the IP trap, we expect for the loss rate due to non adiabatic spin flips an expression similar than the one given by Sukumar and Brink [12] in the case of the IP trap, for $S = 1$:

$$\Gamma_{LZ} \simeq \pi\omega_z e^{-\frac{2\Omega}{\omega_z}}. \quad (21)$$

Again, the exponent scales as $\Omega^{3/2}/\alpha$. For example, for rubidium atoms in $F = 1$ with magnetic gradients of about $100 \text{ G}\cdot\text{cm}^{-1}$, a Rabi frequency above 10 kHz is necessary to avoid Landau-Zener losses (recent measurements at LPL).

In the horizontal direction, the trap is isotropic. The oscillation frequency is imposed by the geometry of the ellipsoid and by gravity: the motion is pendulum-like, with an oscillation frequency in the harmonic approximation of order $\sqrt{g/2r_0}$. More precisely, if we neglect the very small vertical gravitational sag of the potential minimum with respect to the resonant surface, the expression of the horizontal frequency is

$$\omega_\rho \simeq \sqrt{\frac{g}{2r_0}} \left[1 - \frac{\beta\Omega}{\omega}\right]^{1/2}. \quad (22)$$

The correction in $\beta\Omega/\omega$ comes from the vertical dependence of the Rabi frequency. The exact expression is given in the reference [11]. The two values (20) and (22) however give

a very good estimate of the oscillation frequencies. The trap is very anisotropic, and the aspect ratio is approximately

$$\frac{\omega_z}{\omega_\rho} \simeq \alpha \sqrt{\frac{2S\hbar r_0}{Mg\Omega}} = \sqrt{\frac{2S\hbar\alpha\omega}{Mg\Omega}} = \sqrt{\frac{\beta\omega}{\Omega}} > \frac{\omega}{\Omega}. \quad (23)$$

The last inequality is the condition (19) for the trap minimum to be at the bottom of the ellipsoid. We see here that as soon as the rf field fulfills the RWA $\omega \gg \Omega$, the trap is naturally very anisotropic. It has been used to prepare quasi two-dimensional quantum gases [11].

3.5 Linear polarization

If the polarization is chosen to be linear, the best choice is a horizontal polarization, to ensure a maximum coupling at the bottom. Let us choose a polarization \mathbf{e}_x along the x axis. The rf coupling is

$$\begin{aligned} \Omega_+ &= \frac{\Omega}{\sqrt{2\rho\ell}}(2zx - iy). \\ |\Omega_+| &= \Omega \frac{\sqrt{4z^2x^2 + \ell^2y^2}}{\rho\ell} = \Omega \frac{\sqrt{\ell^2\rho^2 - \rho^2x^2}}{\rho\ell} = \Omega \sqrt{1 - \frac{x^2}{\ell^2}}. \end{aligned}$$

Ω is defined as the maximum coupling. If we again assume that the potential minimum will lie on the resonance surface, we end up with

$$V_{\text{surf}}(\mathbf{r}) = S\hbar\Omega \sqrt{1 - \frac{x^2}{r_0^2}} + Mgz, \quad |z| < \frac{r_0}{2}, \quad |x| < r_0, \quad \ell(\rho, z) = r_0.$$

Now, the rotational symmetry is broken by the choice of the rf polarization. There is again a competition between gravity and the coupling gradient, in the $y = 0$ plane where $V_{\text{surf}}(z) = 2S\hbar\Omega z/r_0 + Mgz$. Gravity wins if $\omega > 2\beta\Omega$. This condition is almost the same as in the previous case, and is fulfilled within RWA. For large magnetic gradients, the rf frequency must be increased to fulfill the condition on gravity.

The vertical oscillation frequency at the trap bottom is unchanged with respect to the previous case (20). As the coupling strength is now uniform in the yz plane, the oscillation frequency along y is the bare pendulum frequency:

$$\omega_y = \sqrt{\frac{g}{2r_0}}. \quad (24)$$

The x oscillation frequency is lowered by the attraction to the holes.

$$\omega_x \simeq \sqrt{\frac{g}{2r_0}} \left[1 - \frac{2\beta\Omega}{\omega} \right]^{1/2}. \quad (25)$$

This effect is twice as large as in the circularly polarized case, because the holes are at half the height. The condition on gravity is clear from the expression of the oscillation frequency, which would vanish at the limit $\omega = 2\beta\Omega$ where the single minimum at the

bottom disappear, and the two minima at the equator appear — with zero coupling and strong spin flips.

Here, the important point is that, while the trap is still extremely anisotropic in the vertical versus horizontal directions, it also becomes anisotropic in-plane, with an aspect ratio $\left[1 - \frac{2\beta\Omega}{\omega}\right]^{1/2}$ controlled by the rf amplitude. The direction of this anisotropy is controlled by the polarization axis. In short, modulating the direction of the polarization axis or the rf amplitude allows to set the gas into rotation or excite quadrupole oscillations, respectively. This has been used recently in our group to study collective modes of a two-dimensional superfluid, with an anisotropy of about 1.2 [13]. The smooth character of the adiabatic potential [11, 14] is very well suited for such studies.

How much can we increase the in-plane anisotropy? We remark that the two aspect ratio ω_z/ω_y and ω_x/ω_y are related:

$$\frac{\omega_y}{\omega_z} = \sqrt{\frac{\Omega}{\beta\omega}} \quad \Rightarrow \quad \frac{\omega_x}{\omega_y} = \left[1 - \frac{2\beta\Omega}{\omega}\right]^{1/2} = \left[1 - 2\beta^2 \left(\frac{\omega_y}{\omega_z}\right)^2\right]^{1/2}.$$

For an important in-plane anisotropy, $\beta\omega_y/\omega_z$ should approach $1/\sqrt{2}$. In order to stay in the 2D regime, which requires in particular a strong anisotropy $\omega_z \gg \omega_y$, very large gradients $\beta \gg 1$ are necessary. Experimentally, the in-plane anisotropy which can be obtained thus depends on the maximal feasible gradient.

3.6 Ring trap

Starting from a dressed quadrupole trap with a circular polarization, a ring trap can be obtained by cutting the ellipsoid by a horizontal plane. This can be done with a laser, using the dipole force of a standing wave [15] or of a pair of blue detuned light sheets [16].

The ring radius is easily adjustable dynamically, for example with the frequency ω . On the other hand, using a non circular polarization, with an additional component on x for example, induces a deformation of the ring along x . Rotating the direction of this additional rf component allows to induce a rotation of the atoms in the ring and create a superflow.

4 What is not in this lecture notes

A future version of this lecture notes would include the description of time-averaged adiabatic potentials (TAAP) [17], which have been implemented in the group of Chris Foot [18, 19]. On this subject, I recommend the PhD thesis of Markus Gildemeister, see https://www2.physics.ox.ac.uk/sites/default/files/2013-01-19/dphil_gildemeister_pdf_59116.pdf.

The effects of a strong coupling, beyond the rotating wave approximation, have been investigated in the group of Jörg Schmiedmayer, see [20].

Using another rf frequency is very useful either for performing rf spectroscopy [20, 21] or rf evaporation [22]. Rf spectroscopy allows a determination of the Rabi frequency with an accuracy of below 0.5% [11].

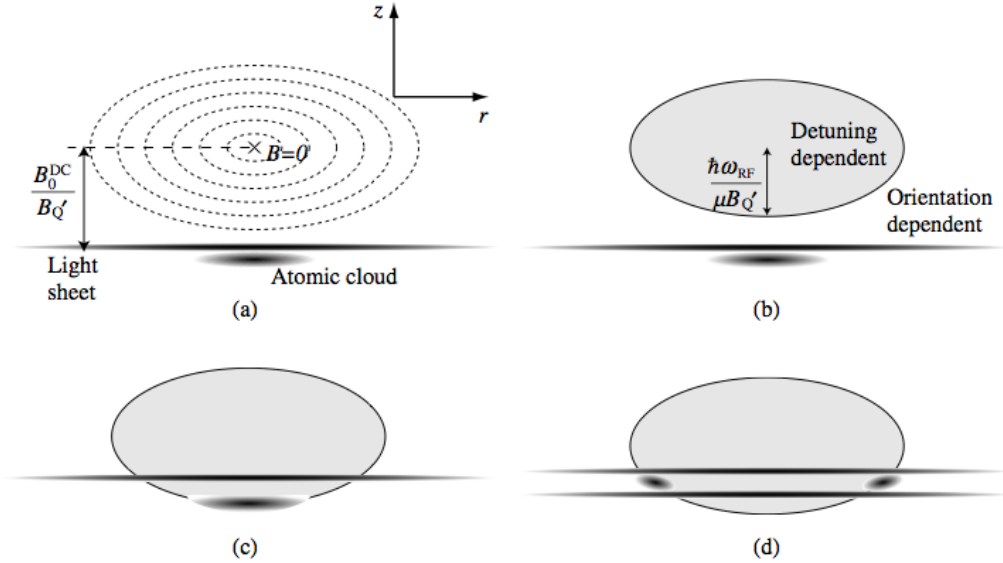


Figure 6: Principle of the ring trap: intersecting a bubble with a plane [16].

References

- [1] A.J. Moerdijk, B.J. Verhaar, and T.M. Nagtegaal. Collisions of dressed ground-state atoms. *Phys. Rev. A*, 53(6):4343–4351, 1996.
- [2] O. Zobay and B.M. Garraway. Two-dimensional atom trapping in field-induced adiabatic potentials. *Phys. Rev. Lett.*, 86(7):1195–1198, 2001.
- [3] O. Zobay and B.M. Garraway. Atom trapping and two-dimensional Bose-Einstein condensates in field-induced adiabatic potentials. *Phys. Rev. A*, 69:023605, 1–15, 2004.
- [4] Y. Colombe, E. Knyazchyan, O. Morizot, B. Mercier, V. Lorent, and H. Perrin. Ultracold atoms confined in rf-induced two-dimensional trapping potentials. *Europhys. Lett.*, 67(4):593–599, 2004.
- [5] O. Morizot. *Pièges radiofréquence très anisotropes pour un condensat de Bose-Einstein*. PhD thesis, Université Paris XIII, 2007.
- [6] Y. Colombe. *Condensat de Bose-Einstein, champs évanescents et piégeage bidimensionnel*. PhD thesis, Université Paris XIII, 2004.
- [7] O. Morizot, L. Longchambon, R. Kollengode Easwaran, R. Dubessy, E. Knyazchyan, P.-E. Pottie, V. Lorent, and H. Perrin. Influence of the Radio-Frequency source properties on RF-based atom traps. *Eur. Phys. J. D*, 47:209, 2008.
- [8] I. Lesanovsky, T. Schumm, S. Hofferberth, L. M. Andersson, P. Krüger, J. Schmiedmayer. Adiabatic radio frequency potentials for the coherent manipulation of matter waves. *Phys. Rev. A*, 73:033619, 2006.

- [9] T. Schumm, S. Hofferberth, L.M. Andersson, S. Wildermuth, S. Groth, I. Bar-Joseph, J. Schmiedmayer, and P. Krüger. Matter wave interferometry in a double well on an atom chip. *Nature Phys.*, 1:57, 2005.
- [10] O. Morizot, C.L. Garrido Alzar, P.-E. Pottie, V. Lorent, and H. Perrin. Trapping and cooling of rf-dressed atoms in a quadrupole magnetic field. *J. Phys. B: At. Mol. Opt. Phys.*, 40:4013–4022, 2007.
- [11] K. Merloti, R. Dubessy, L. Longchambon, A. Perrin, P.-E. Pottie, V. Lorent, and H. Perrin. A two-dimensional quantum gas in a magnetic trap. *New Journal of Physics*, 15(3):033007, 2013.
- [12] D.M. Brink and C.V. Sukumar. Majorana spin-flip transitions in a magnetic trap. *Phys. Rev. A*, 74(3):035401, 2006.
- [13] K. Merloti. *Condensat de Bose-Einstein dans un piège quadrupolaire habillé: modes collectifs d'un gaz bidimensionnel*. PhD thesis, Université Paris XIII, 2013.
- [14] J. J. P. van Es, S. Whitlock, T. Fernholz, A. H. van Amerongen, and N. J. van Druten. Longitudinal character of atom-chip-based rf-dressed potentials. *Phys. Rev. A*, 77:063623, Jun 2008.
- [15] O. Morizot, Y. Colombe, V. Lorent, H. Perrin, and B.M. Garraway. Ring trap for ultracold atoms. *Phys. Rev. A*, 74:023617, 2006.
- [16] W. H. Heathcote, E. Nugent, B. T. Sheard, and C. J. Foot. A ring trap for ultracold atoms in an rf-dressed state. *New Journal of Physics*, 10(4):043012, 2008.
- [17] I. Lesanovsky and W. von Klitzing. Time-Averaged Adiabatic Potentials: Versatile Matter-Wave Guides and Atom Traps. *Phys. Rev. Lett.*, 99:083001, 2007.
- [18] M. Gildemeister, E. Nugent, B. E. Sherlock, M. Kubasik, B. T. Sheard, and C. J. Foot. Trapping ultracold atoms in a time-averaged adiabatic potential. *Phys. Rev. A*, 81:031402, Mar 2010.
- [19] B. E. Sherlock, M. Gildemeister, E. Owen, E. Nugent, and C. J. Foot. Time-averaged adiabatic ring potential for ultracold atoms. *Phys. Rev. A*, 83:043408, Apr 2011.
- [20] S. Hofferberth, B. Fischer, T. Schumm, J. Schmiedmayer, and I. Lesanovsky. Ultracold atoms in radio-frequency dressed potentials beyond the rotating-wave approximation. *Phys. Rev. A*, 76:013401, Jul 2007.
- [21] R. Kollengode Easwaran, L. Longchambon, P.-E. Pottie, V. Lorent, H. Perrin, and B. M. Garraway. RF spectroscopy in a resonant RF-dressed trap. *Journal of Physics B: Atomic, Molecular and Optical Physics*, 43(6):065302, 2010.
- [22] C.L. Garrido Alzar, H. Perrin, B.M. Garraway, and V. Lorent. Evaporative cooling in a radio-frequency trap. *Phys. Rev. A*, 74:053413, 2006.